High-Resolution X-ray Computed Tomography of Macroporous Karst for Permeability Measurement and Non-Darcian Flow via Lattice Boltzmann Models

Mike Sukop[1], Haibo Huang[2], Kevin Cunningham[3], and Peter Alvarez[1]

[1]Florida International University
[2]University of Science and Technology of China
[3]United States Geological Survey, Ft. Lauderdale

National Science Foundation
WHERE DISCOVERIES BEGIN

FIU
FLORIDA INTERNATIONAL UNIVERSITY
Miami's public research university

USGS
science for a changing world

Objectives

- Compute K of highly macroporous karst rock
- Compute K under different hydraulic gradients (different Re). Expect reduced apparent K at high Re due to eddy head dissipation

Introduction

- LBM is a mesoscopic method based on the scale between molecular dynamics and familiar continuum approaches
- A particle stream-and-collide perspective with interparticle forces is adequate for most simulations
- LBMs handle complex geometries well

Kinetic Theory

- Complete set of position (**x**) and momentum (**p**) coordinates for all particles gives dynamical state of system
- Together with classical mechanics, allows prediction of future states
- However, this level of description is not possible
- Use a statistical description: focus on the distribution function of the "state" of molecules

$$f(\mathbf{x}, \mathbf{p}, t)$$

LBM Basics

D2Q9

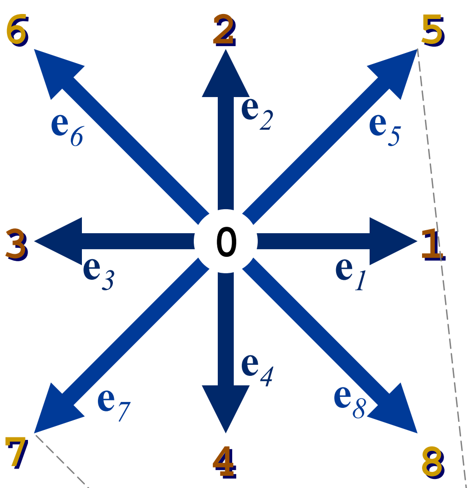

Discrete Velocities $\mathbf{e}_a$

Directional densities f_a

Histogram view of the *distribution function, f.*

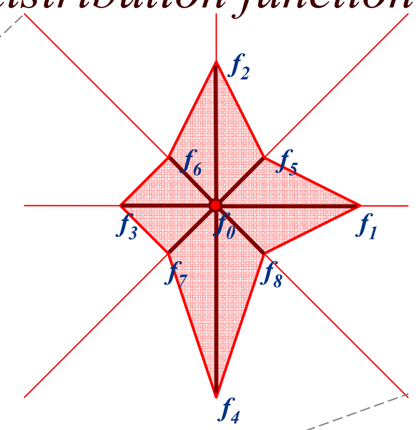

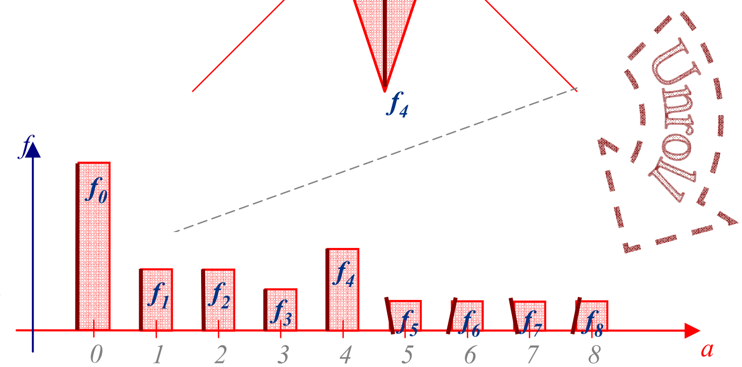

Lattice Unit, *lu*

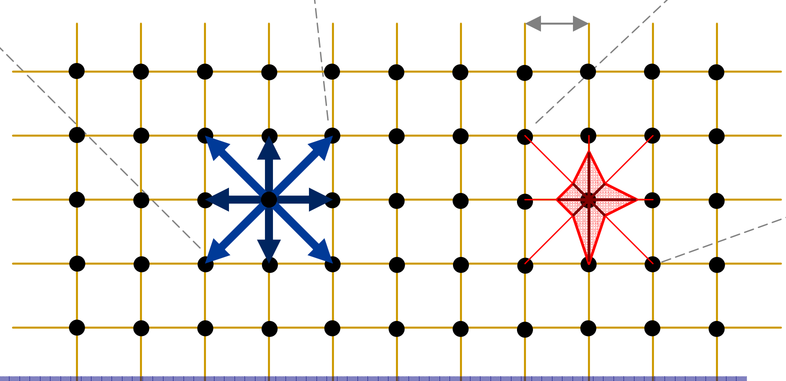

$$\text{Macroscopic density} \quad \rho = \sum_{a=0}^{8} f_a$$

$$\text{Macroscopic velocity} \quad \mathbf{u} = \frac{1}{\rho}\sum_{a=0}^{8} f_a \mathbf{e}_a$$

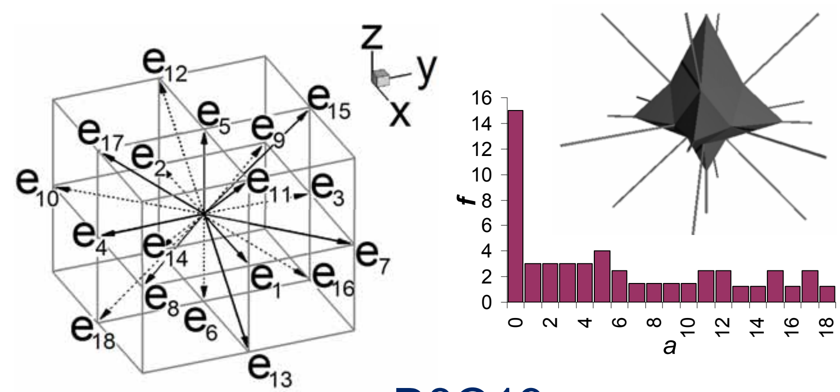

D3Q19

Streaming

$$f_a\left(\mathbf{x}+\mathbf{e}_a\Delta t, t+\Delta t\right)=f_a\left(\mathbf{x},t\right)$$

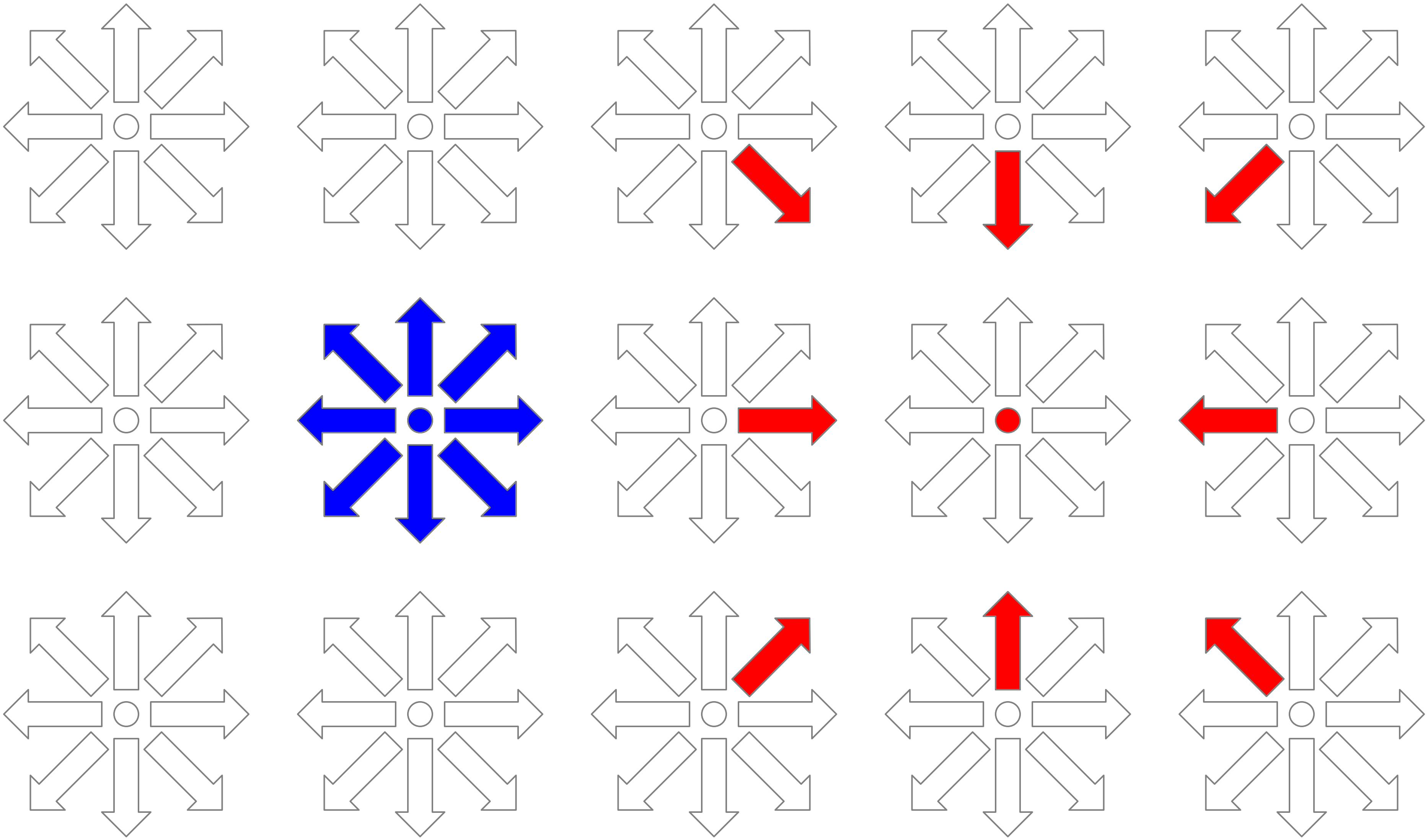

Single Relaxation Time BGK (Bhatnagar-Gross-Krook) Approximation

$$\underbrace{f_a(\mathbf{x}+\mathbf{e}_a\Delta t, t+1) = f_a(\mathbf{x},t) - \underbrace{\frac{\left[f_a(\mathbf{x},t) - f_a^{eq}(\mathbf{x},t)\right]}{\tau}}_{\textbf{Collision (i.e., relaxation towards equilibrium)}}}_{\textbf{Streaming}}$$

$$f_a^{eq}(\mathbf{x}) = w_a \rho(\mathbf{x})\left[1 + 3\frac{\mathbf{e}_a \bullet \mathbf{u}}{c^2} + \frac{9}{2}\frac{(\mathbf{e}_a \bullet \mathbf{u})^2}{c^4} - \frac{3}{2}\frac{\mathbf{u}^2}{c^2}\right]$$

Collision and streaming steps must be separated if solid boundaries present (bounce back boundary is a separate collision)

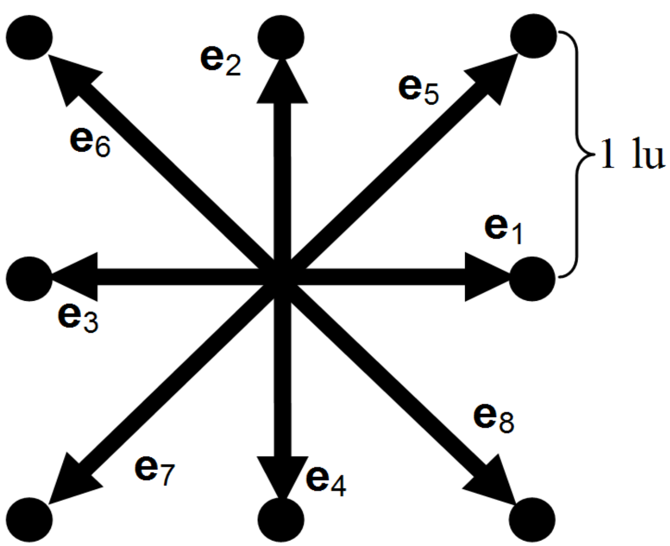

- τ relaxation time (viscosity and diffusion)
- c speed on lattice (1 lu /time step)

- w_a are 4/9 for the rest particles (a = 0),
- 1/9 for a = 1, 2, 3, 4, and
- 1/36 for a = 5, 6, 7, 8.

Poiseuille flow in a circular pipe

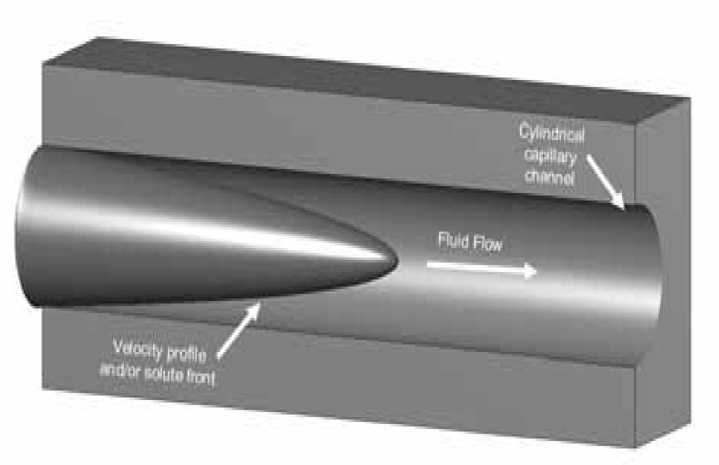

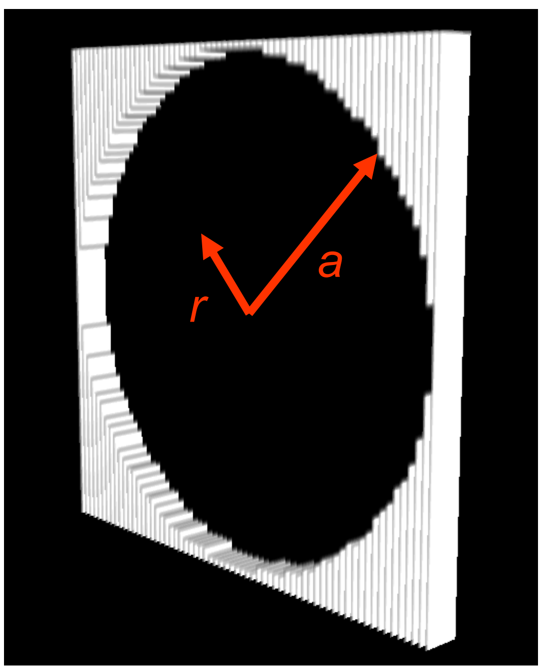

u_x

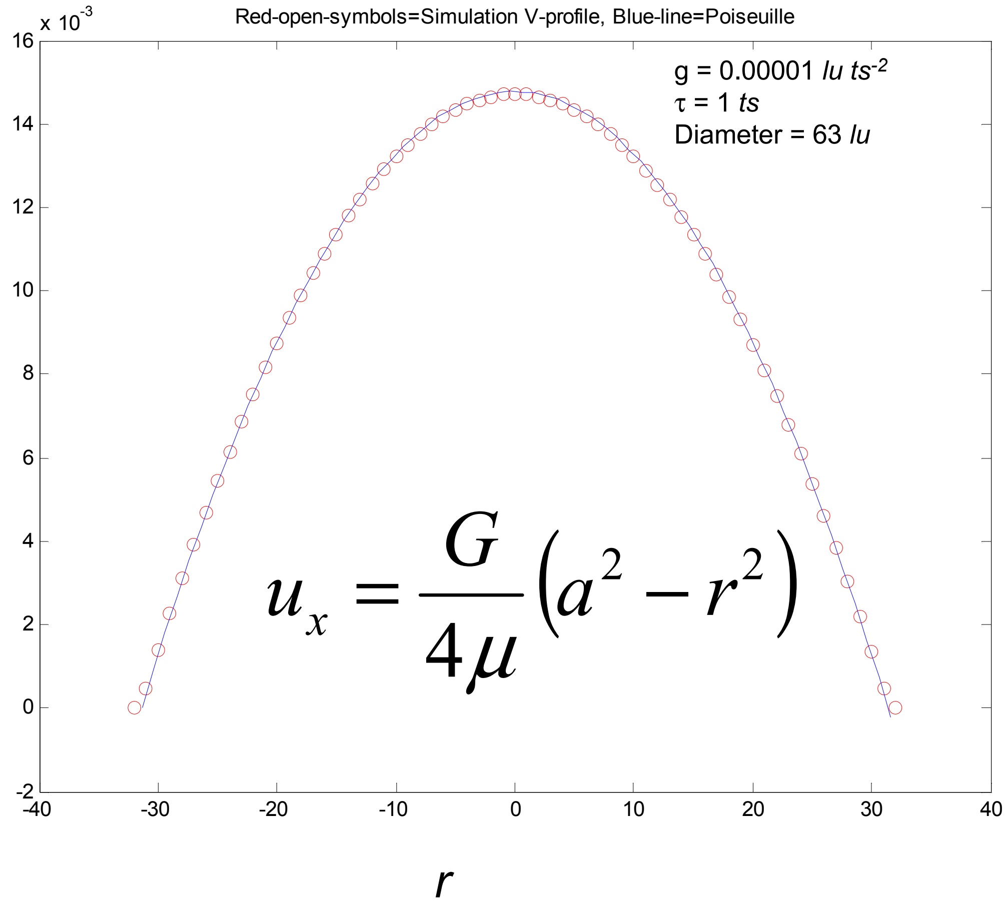

$$u_x = \frac{G}{4\mu}\left(a^2 - r^2\right)$$

Poiseuille flow in a rectangular duct

$$u_x(y,z) = -\frac{1}{2\mu}\frac{\partial p}{\partial x}a^2\left[1-\left(\frac{z}{a}\right)^2 + 4\sum_{k=1}^{\infty}\frac{(-1)^k}{\alpha_k^3}\frac{\cosh\left(\frac{\alpha_k y}{a}\right)}{\cosh\left(\frac{\alpha_k b}{a}\right)}\cos\left(\frac{\alpha_k z}{a}\right)\right]$$

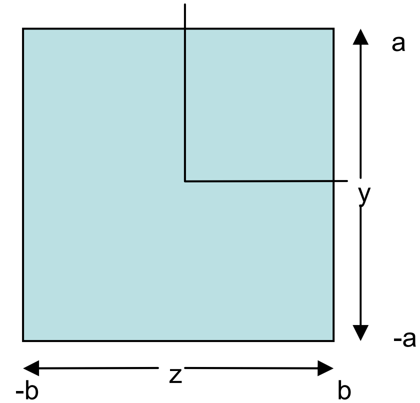

$$\alpha_k = (2k-1)\frac{\pi}{2}, \qquad k = 1, 2, \ldots$$

Papanastasiou, T. C., Georgiou, G. C. , Alexandrou, A. N., (2000). Viscous fluid flow. CRC Press, Boca Raton, p.259

For square, a = b

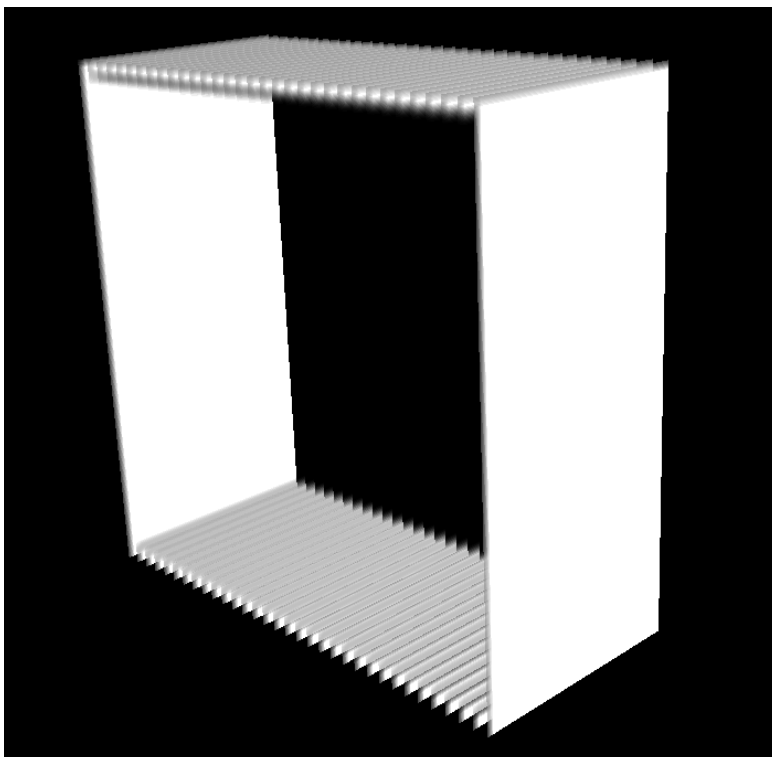

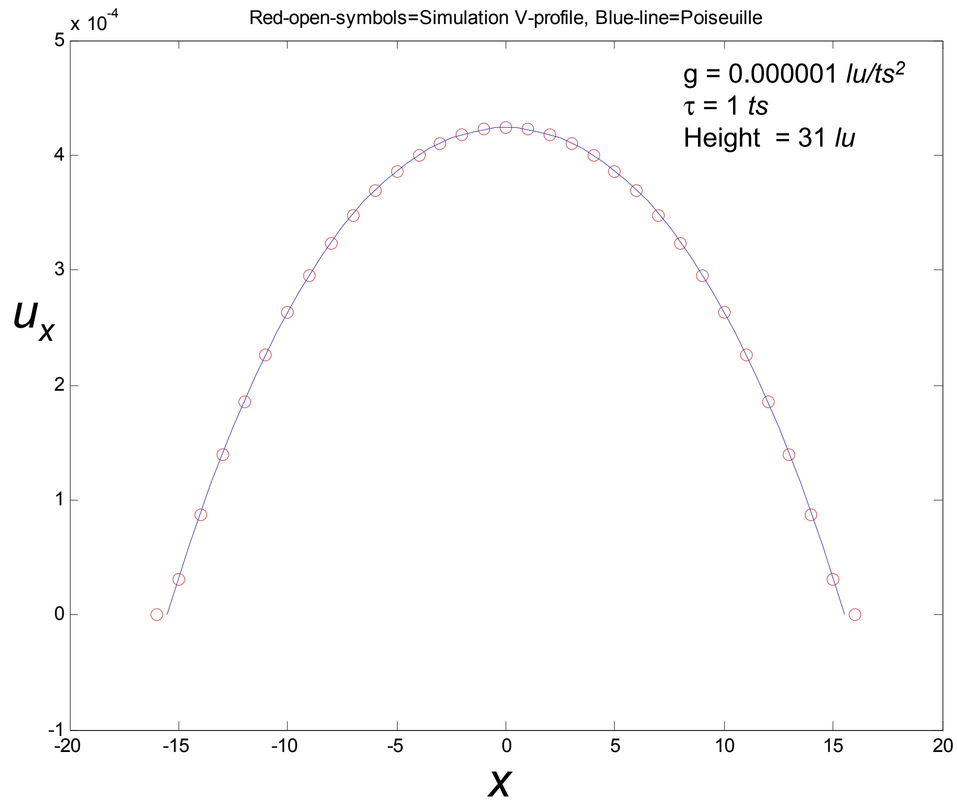

Why use LBM in macroporous karst context?

- Easy to incorporate complex geometry
- Transition to higher Reynolds numbers

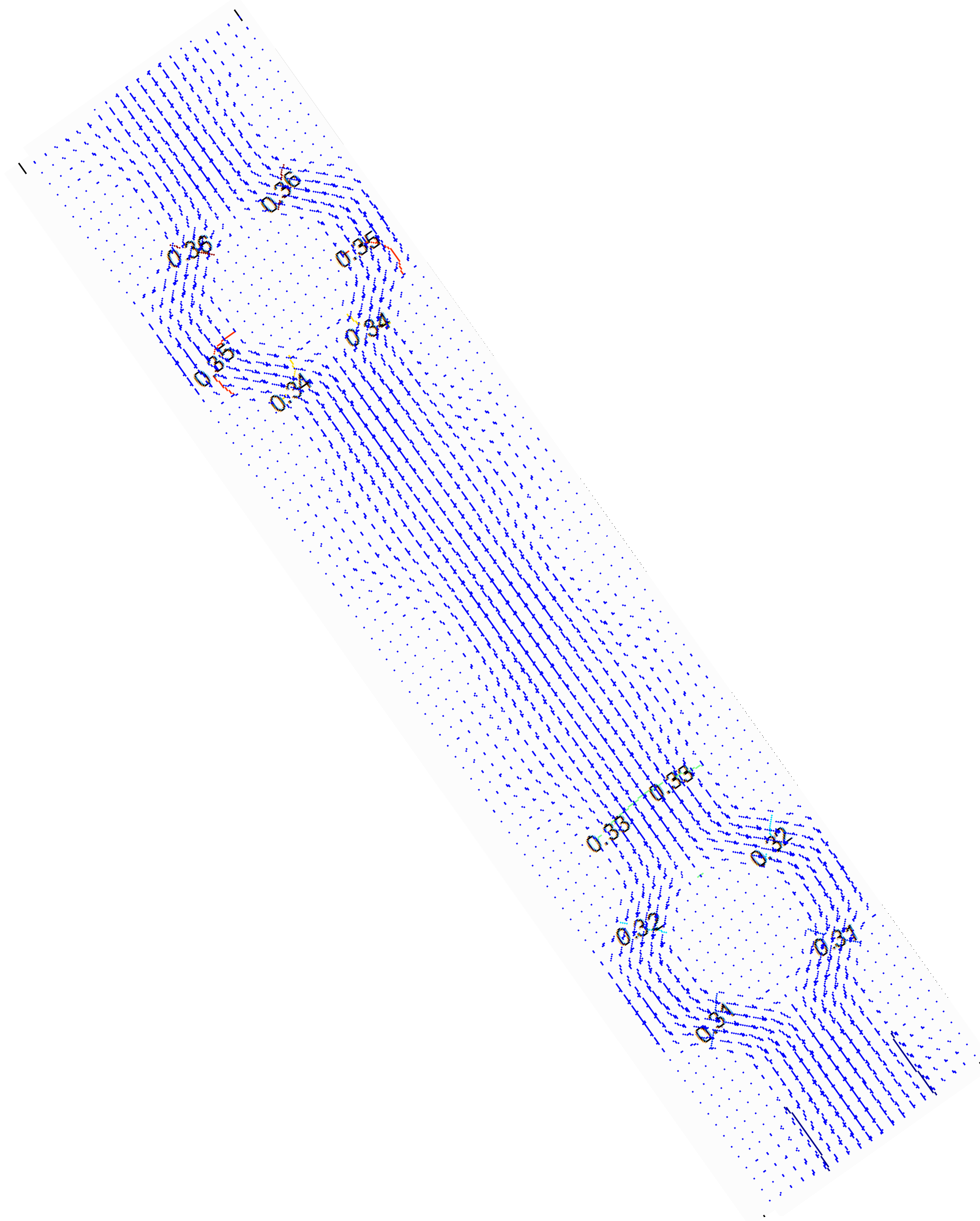

Why use LBM in macroporous karst context?

- Easy to incorporate complex geometry
- Transition to higher Reynolds numbers

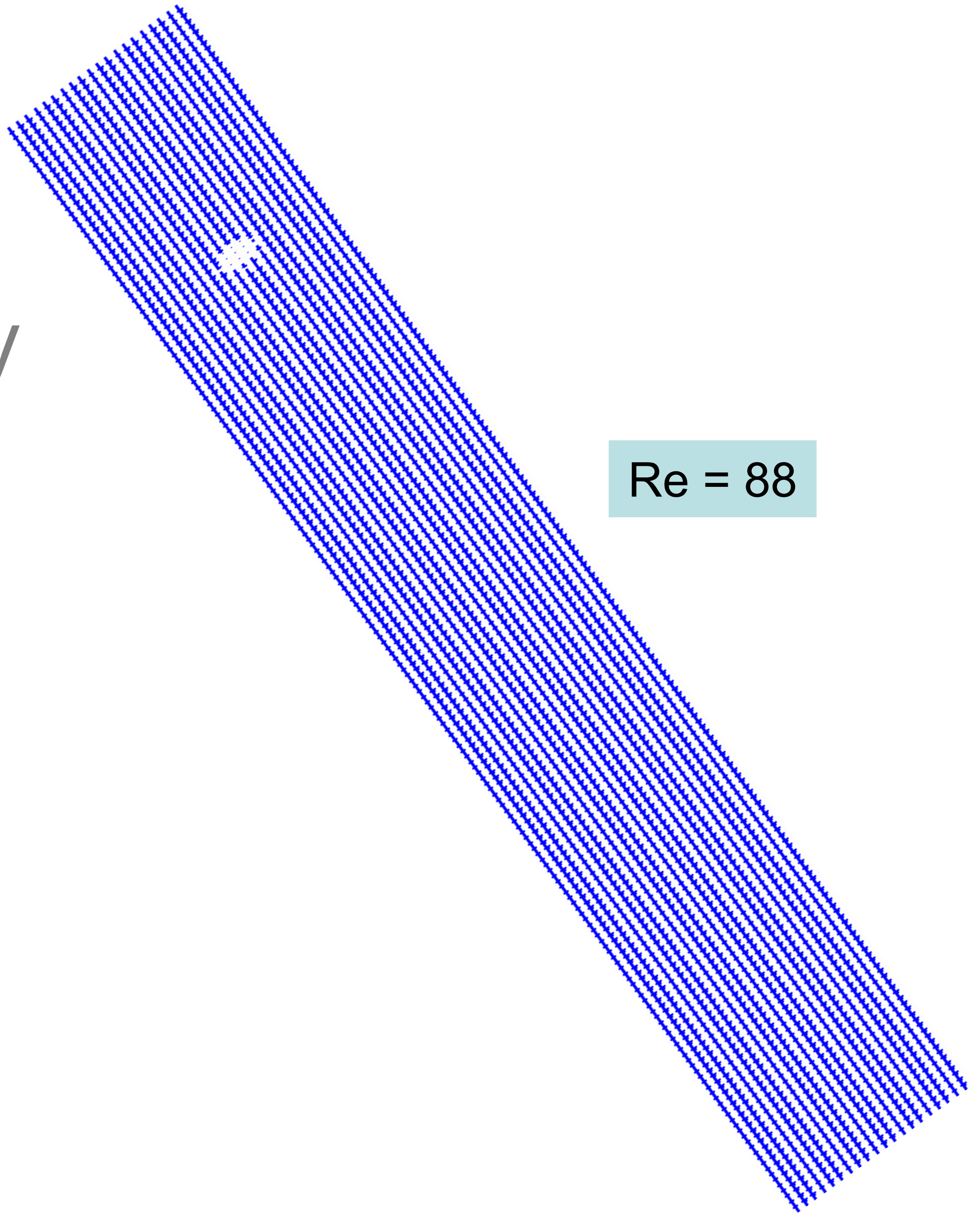

Data and Tools

- Karst data scales
  - 0.0003 to 0.3 m high-resolution CT scans
  - 0.002 to 30 m borehole imagery
  - 1 to 1000 m cave diver sonic rangefinder data
- Medium simulation required for borehole and rangefinder data
- LBM integrative tool
  - Compute K at multiple scales
  - Assess non-Darcy potential and impacts

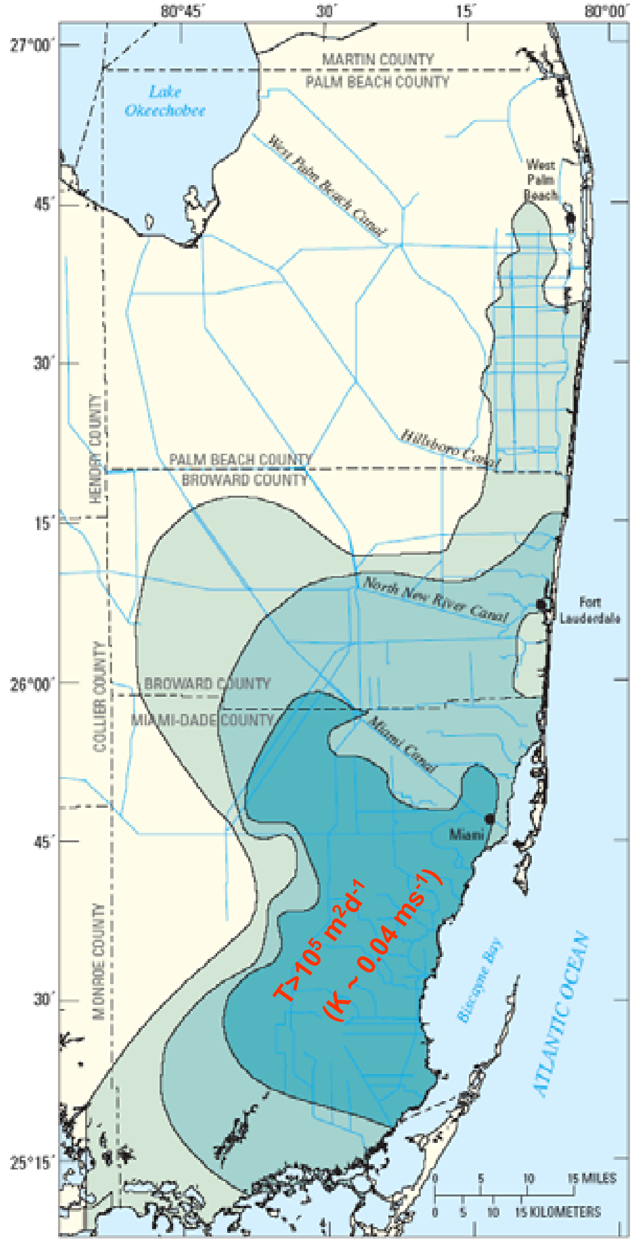

Figure 10. Distribution of transmissivity within the surficial aquifer system in southeastern Florida. Modified from Fish (1988), Shine and others (1989), and Fish and Stewart (1991).

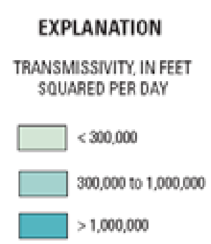

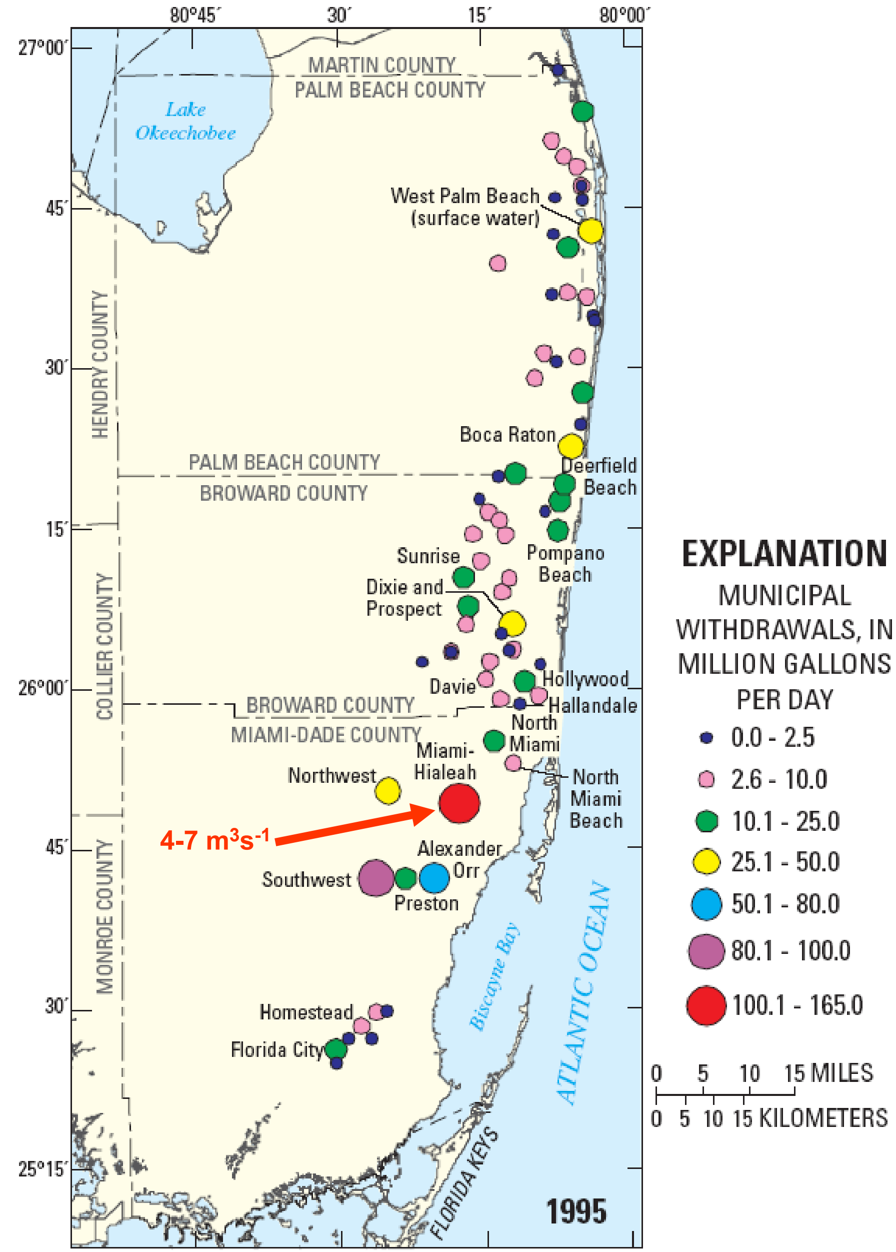

Renken, R.A., Dixon, J., Koehmstedt, J., Lietz, A.C., Ishman, S., Marella, R.L., Telis, P., Rogers, J., and Memberg, S., 2005, Impact of Anthropogenic Development on Coastal Ground-Water Hydrology in Southeastern Florida, 1900-2000: Reston, Va., U.S. Geological Survey Circular 1275, 77 p.

Geology to model parameters

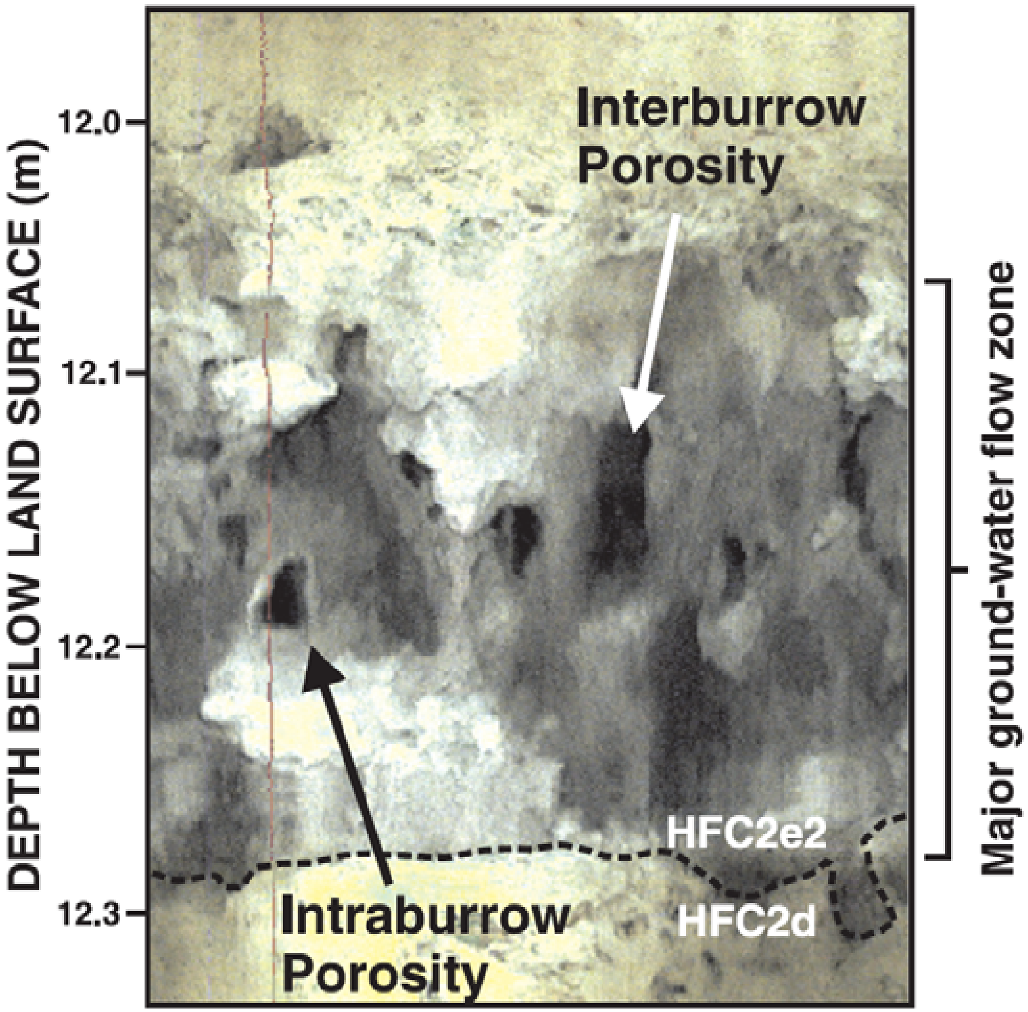

GSA Special Paper 404, 2006

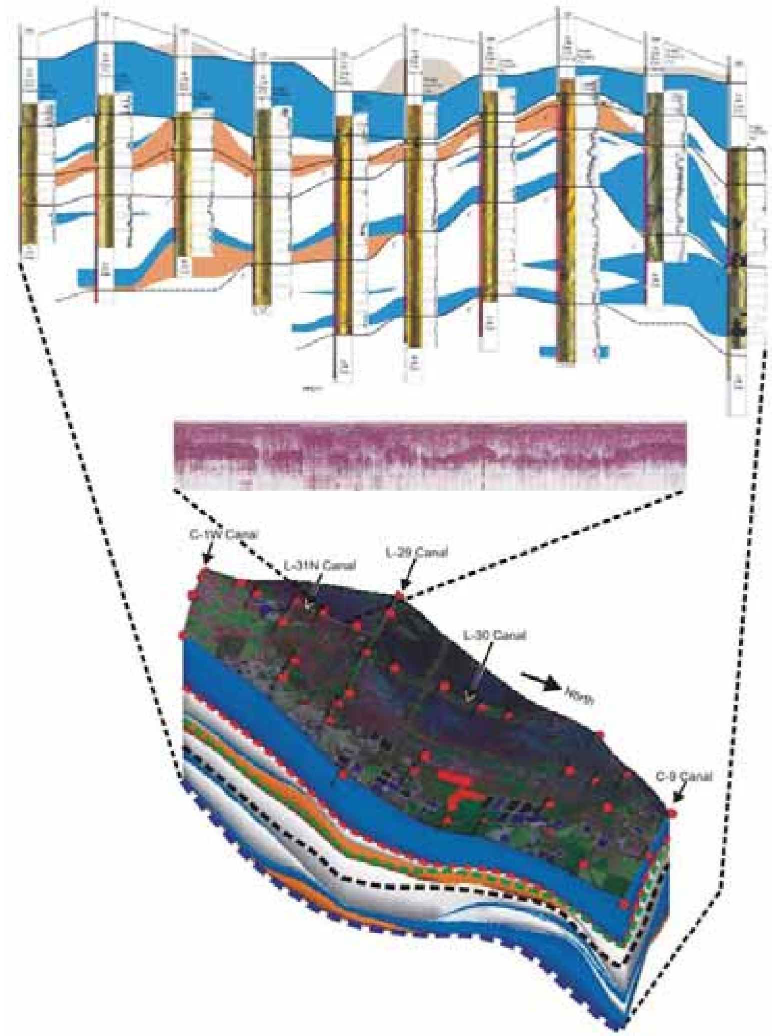

Characterization of Aquifer Heterogeneity Using Cyclostratigraphy and Geophysical Methods in the Upper Part of the Karstic Biscayne Aquifer, Southeastern Florida *By* Kevin J. Cunningham, Janine L. Carlson, G. Lynn Wingard, Edward Robinson, *and* Michael A. Wacker U.S. Geological Survey Water-Resources Investigations Report 03-4208

Example Data Set

Photo: Mike Wacker/USGS

Burrow porosity in Miami Limestone barrier bar deposited during the last interglacial

(maximum unit thickness ~ 1m)

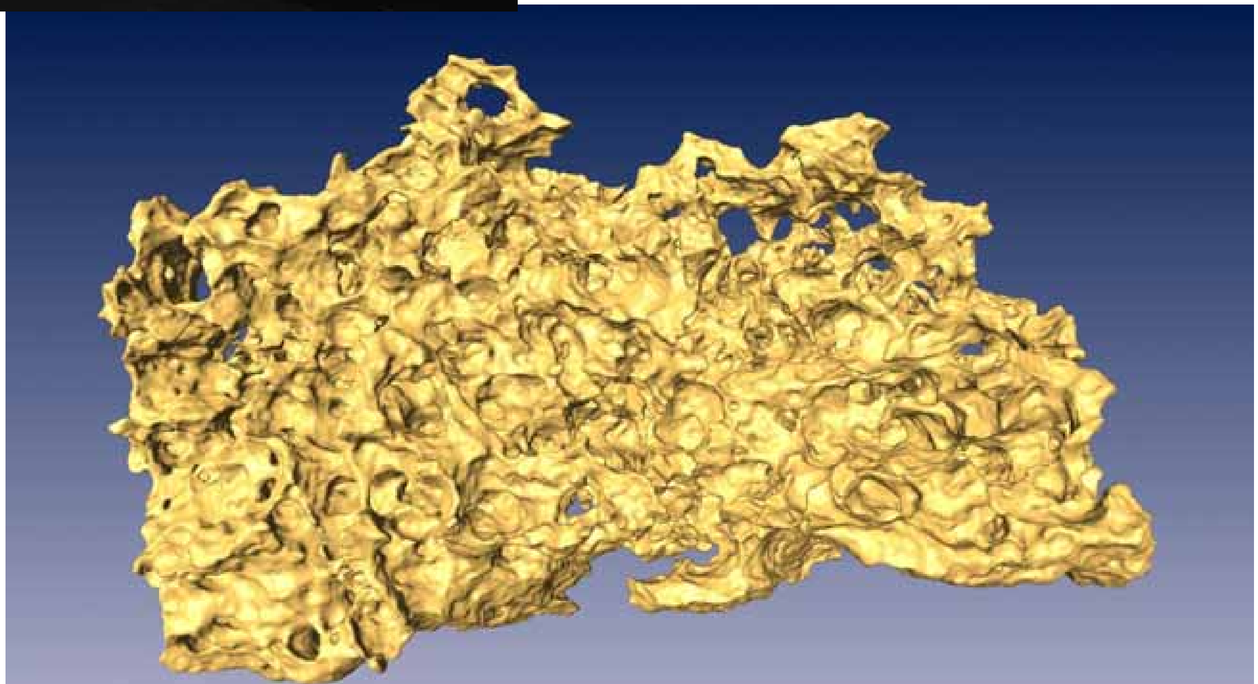

Data and image produced at the High-Resolution X-ray Computed Tomography Facility of the University of Texas at Austin

8- and 16-bit slices

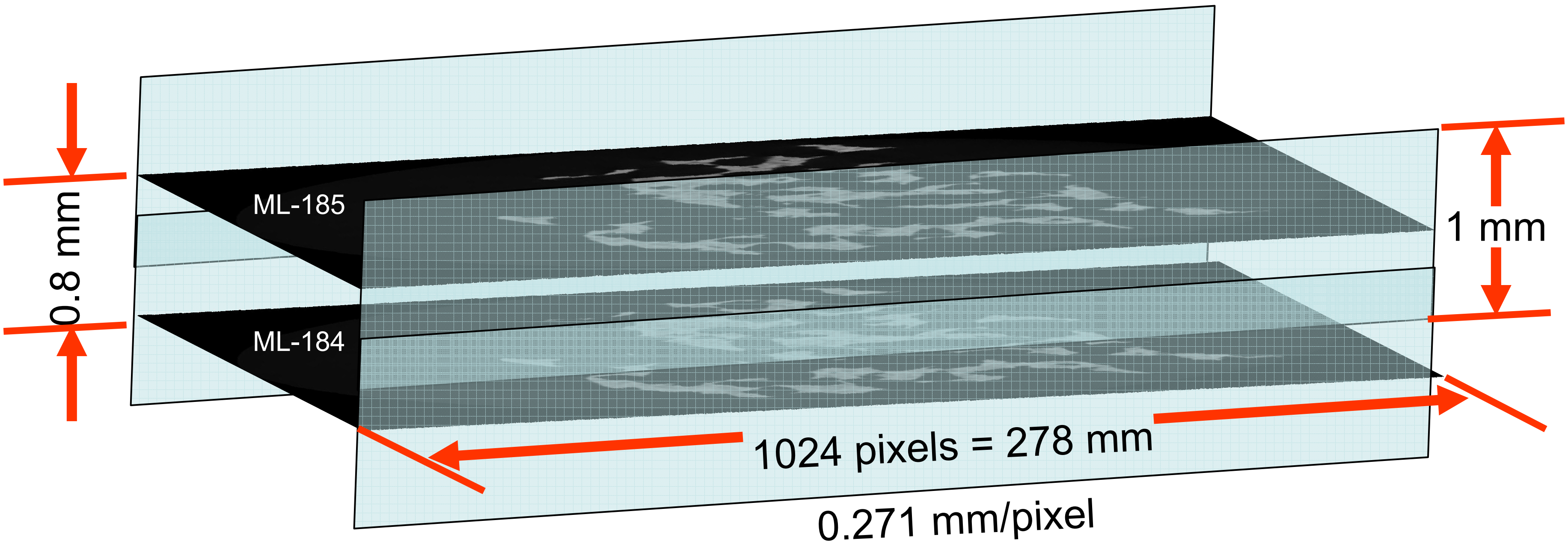

- With 0.8 mm slice spacing, 401 slices = 321 mm

Data and image produced at the High-Resolution X-ray Computed Tomography Facility of the University of Texas at Austin

Thresholding (<75/255 →pore)

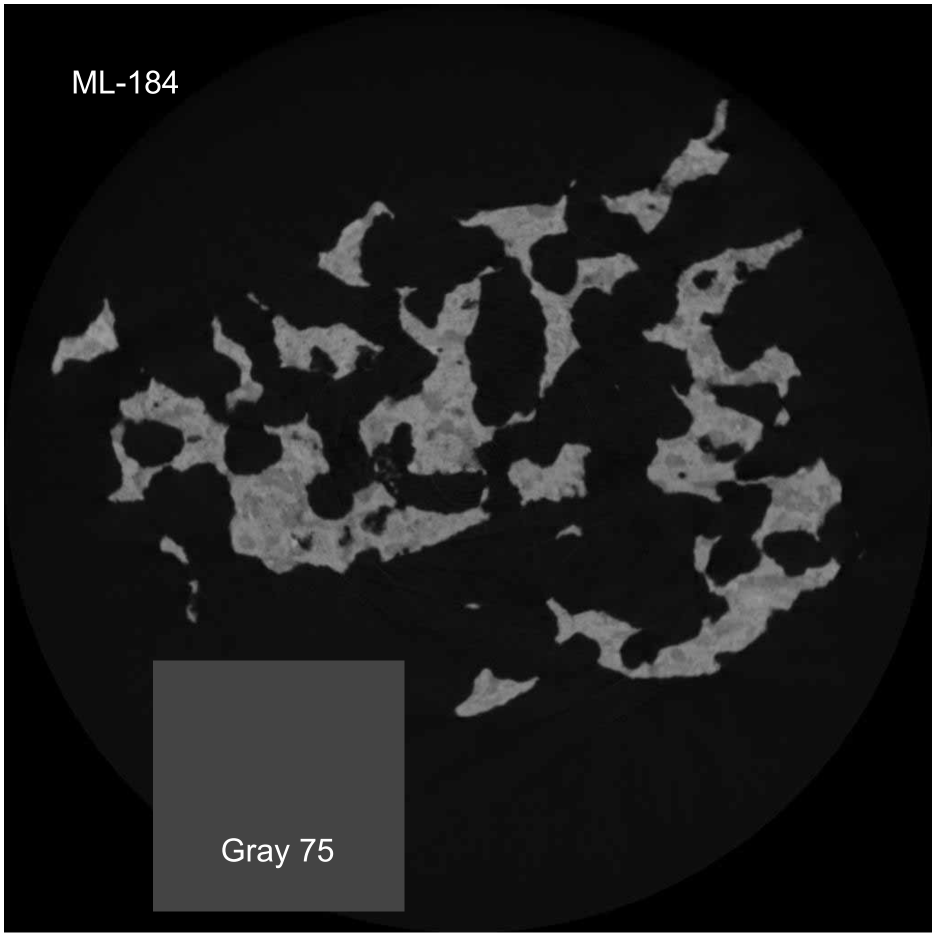

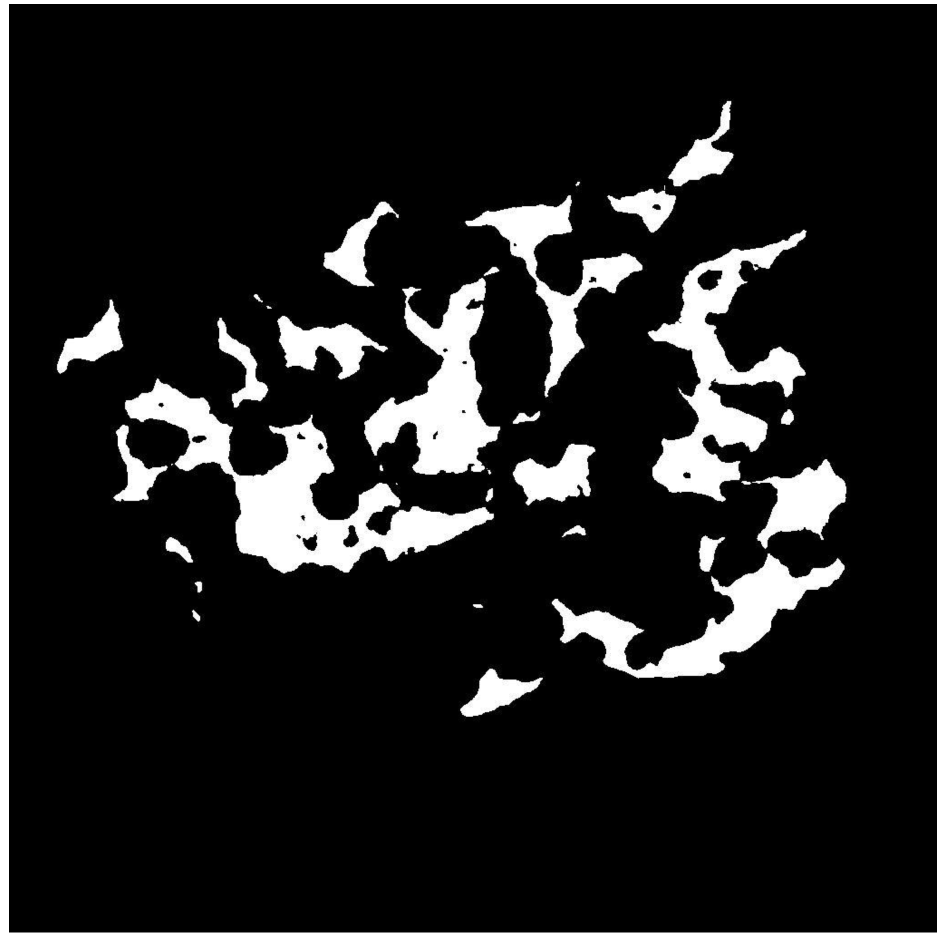

Data and image produced at the High-Resolution X-ray Computed Tomography Facility of the University of Texas at Austin

Bulk of Sample and Experimental Cube

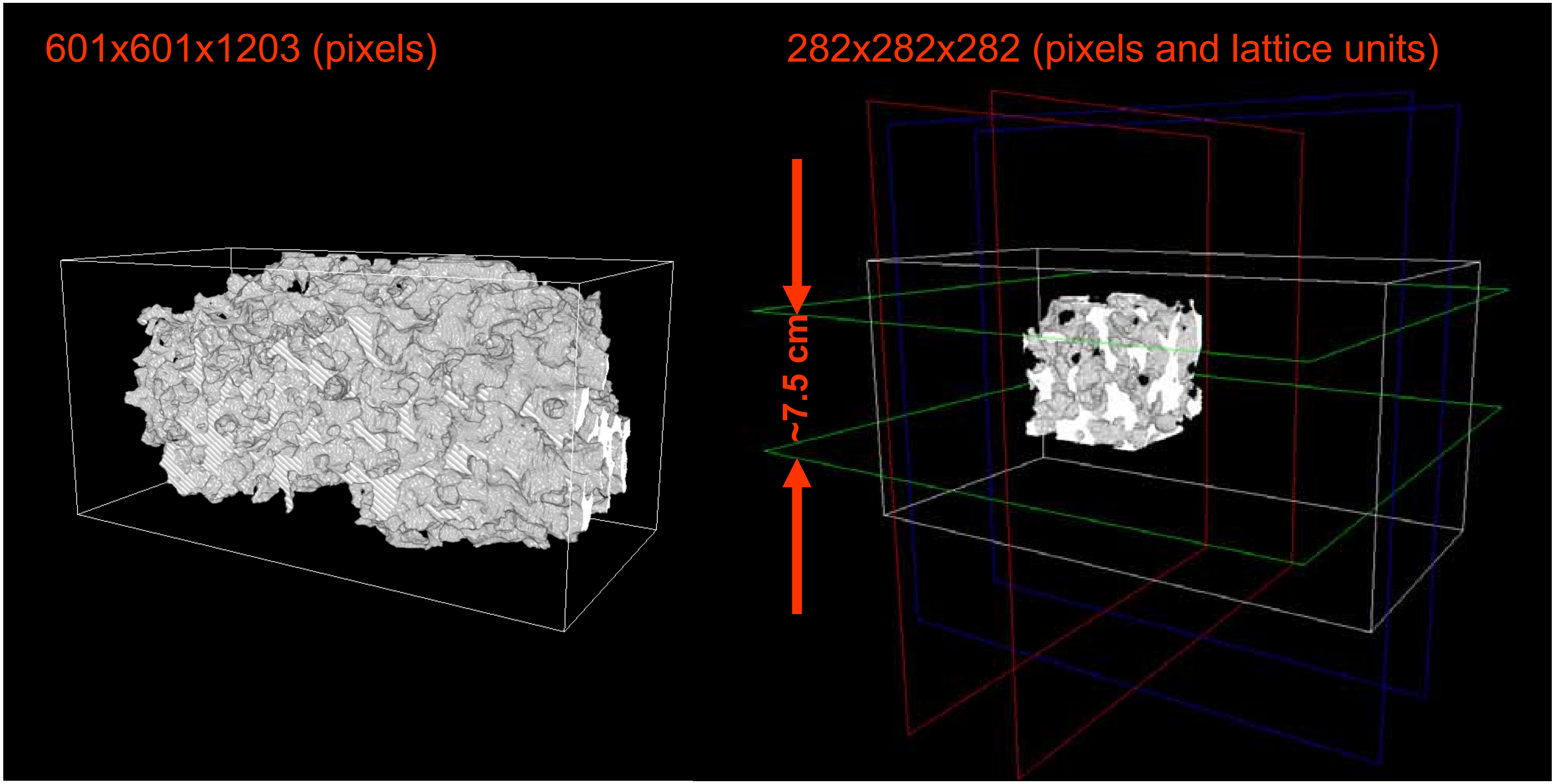

~22 million cells. Limit set by memory of computer and code.

Data produced at the High-Resolution X-ray Computed Tomography Facility of the University of Texas at Austin

Velocity Magnitude

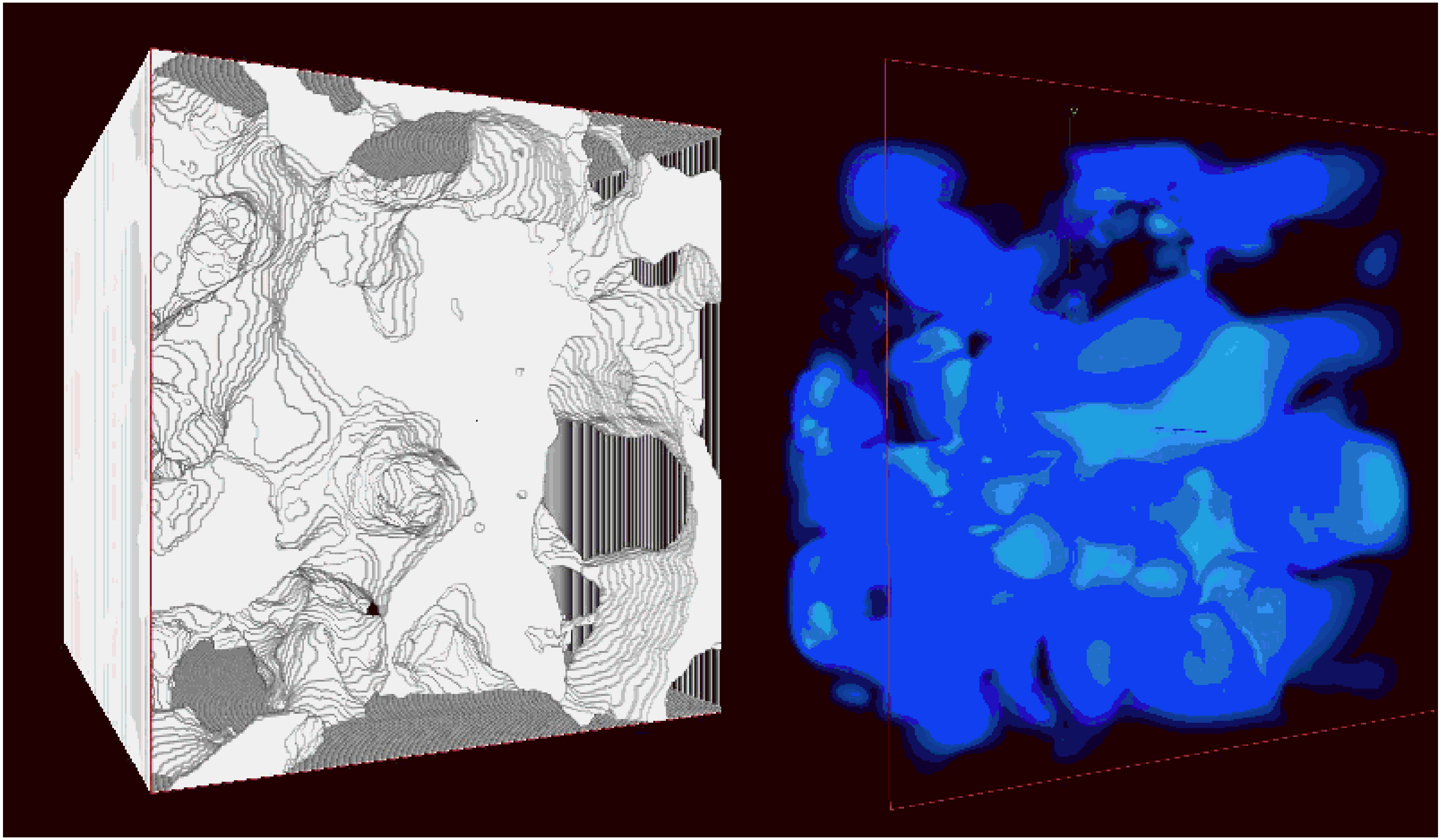

Data produced at the High-Resolution X-ray Computed Tomography Facility of the University of Texas at Austin

Darcy's Law

$$\mathbf{q} = -\mathbf{K}\nabla h$$

- h head (= $p/\rho\mathbf{g}$)
- **K** hydraulic conductivity (LT^{-1})

$$\mathbf{q} = -\mathbf{k}\frac{\rho\mathbf{g}}{\mu}\nabla h$$

$$\mathbf{q} = -\mathbf{k}\frac{1}{\mu}\nabla p$$

- **q** flux
- **k** permeability
- ρ density
- μ viscosity
- p pressure
- **g** gravity

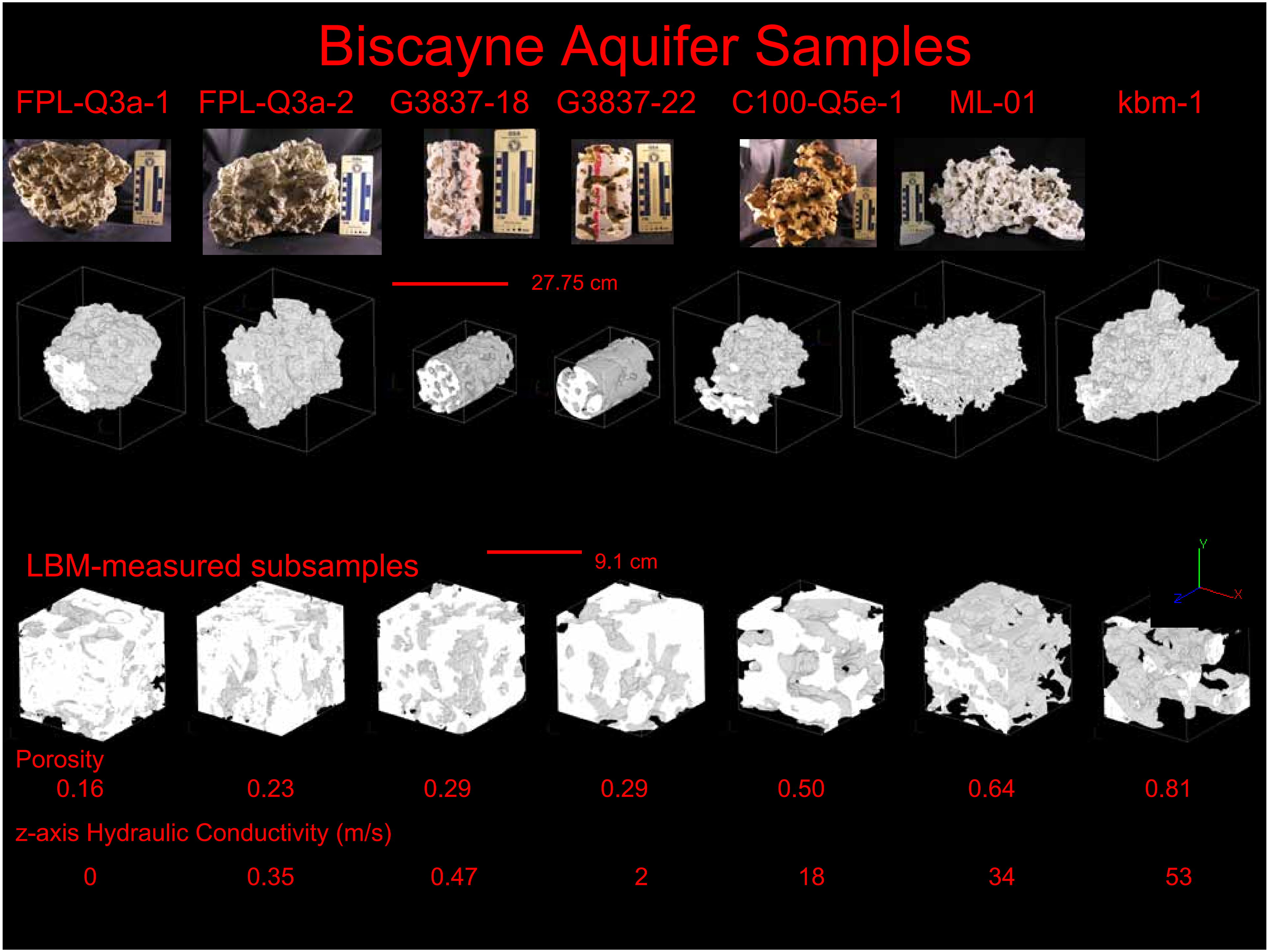
Biscayne Aquifer Samples
FPL-Q3a-1
FPL-Q3a-2
G3837-18
G3837-22
C100-Q5e-1
ML-01
kbm-1
27.75 cm
LBM-measured subsamples
9.1 cm
Y
X
Z
Porosity
0.16
0.23
0.29
0.29
0.50
0.64
0.81
z-axis Hydraulic Conductivity (m/s)
0
0.35
0.47
2
18
34
53

Hydraulic Conductivity Values

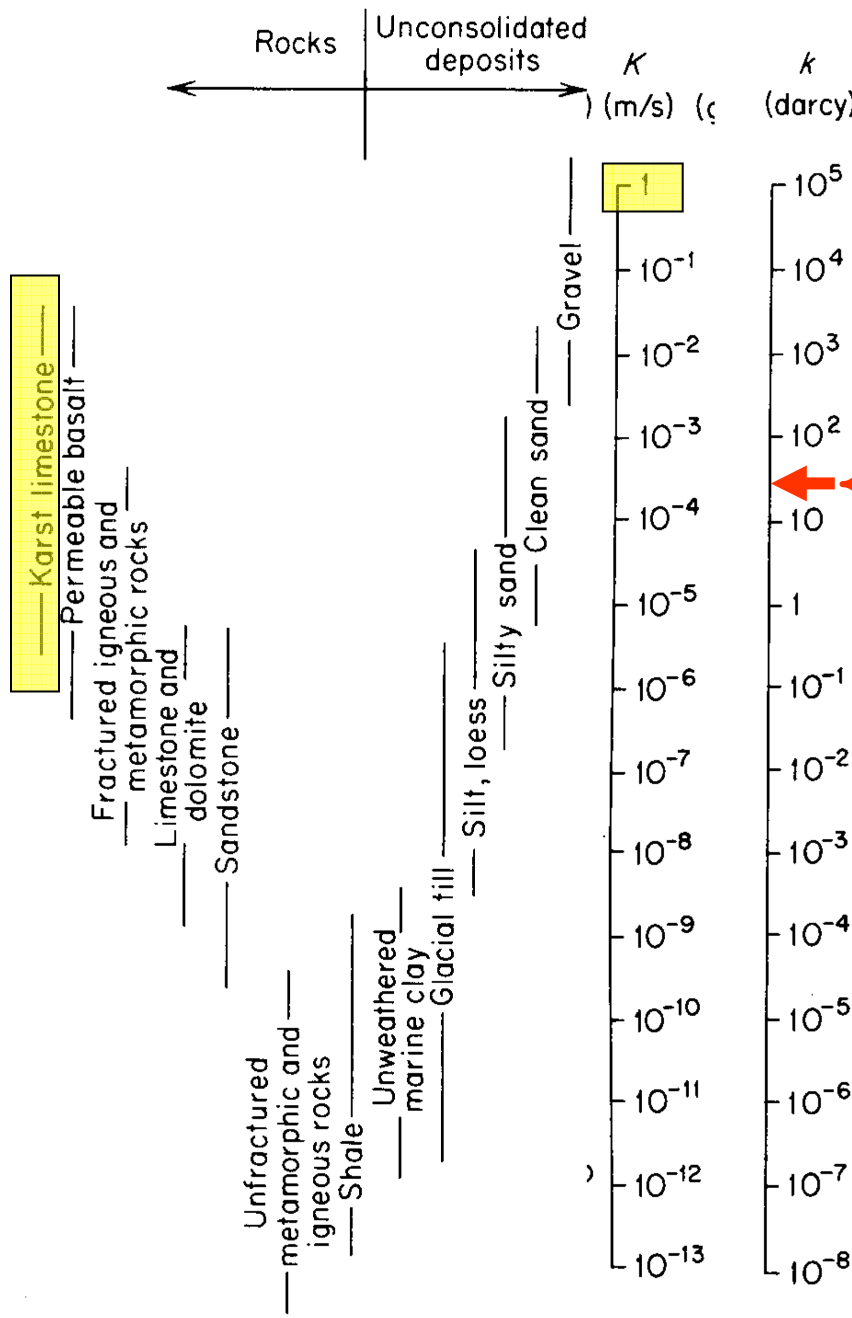

Maximum k from air permeability laboratory measurements

(Cunningham et.al., 2006)

Freeze and Cherry (1979) Groundwater, Prentice-Hall

Darcy-Forschheimer Equation

- Darcy:

$$\frac{\mu}{\mathbf{k}}\mathbf{q} = -\nabla p$$

- +Non-linear drag term:

$$\frac{\mu}{\mathbf{k}}\mathbf{q} + \boxed{a|\mathbf{q}|\mathbf{q}} = -\nabla p$$

Apparent K as a function of hydraulic gradient

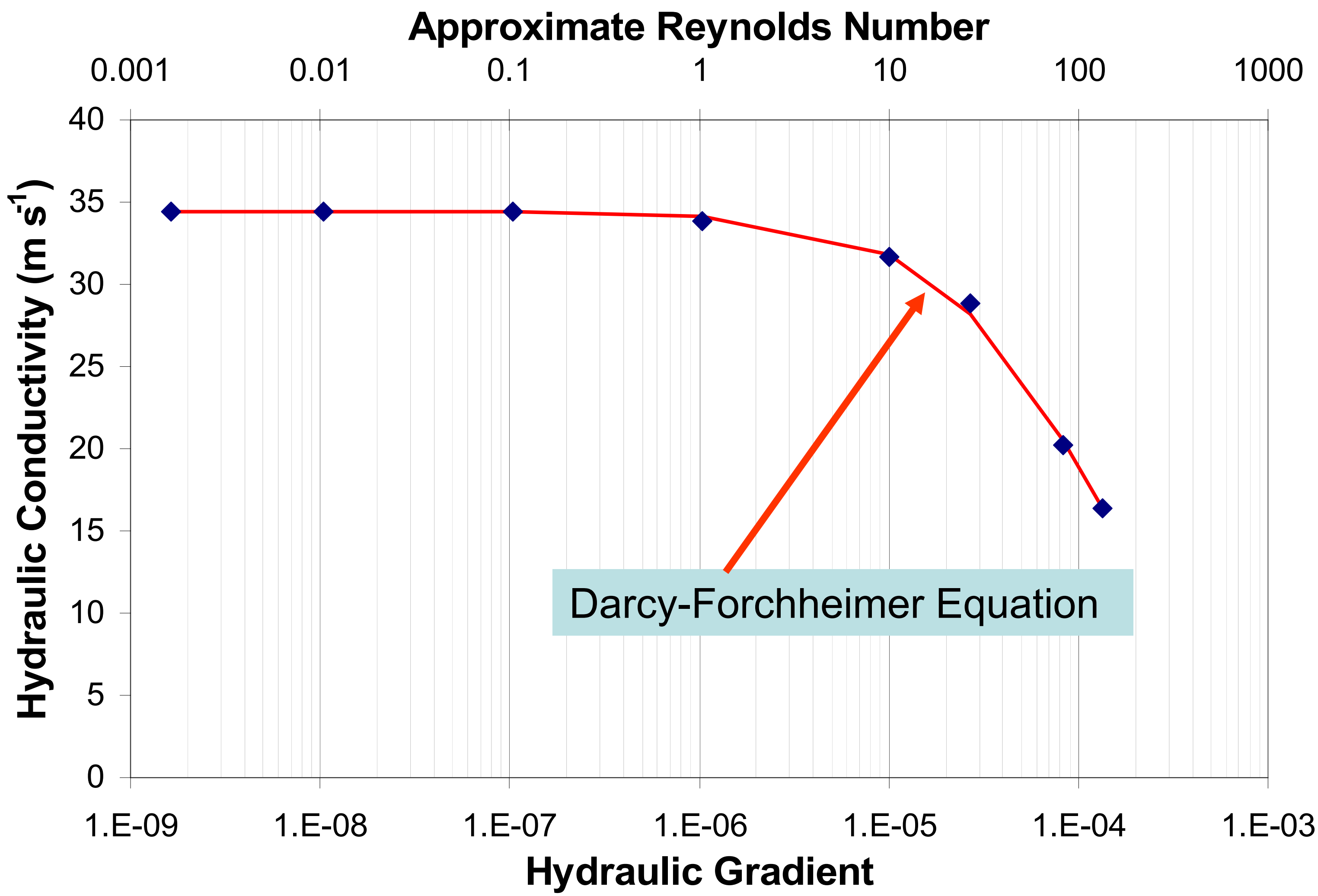

- Gradients could be higher locally
- Expect leveling at higher gradient?

Streamlines at different Reynolds Numbers

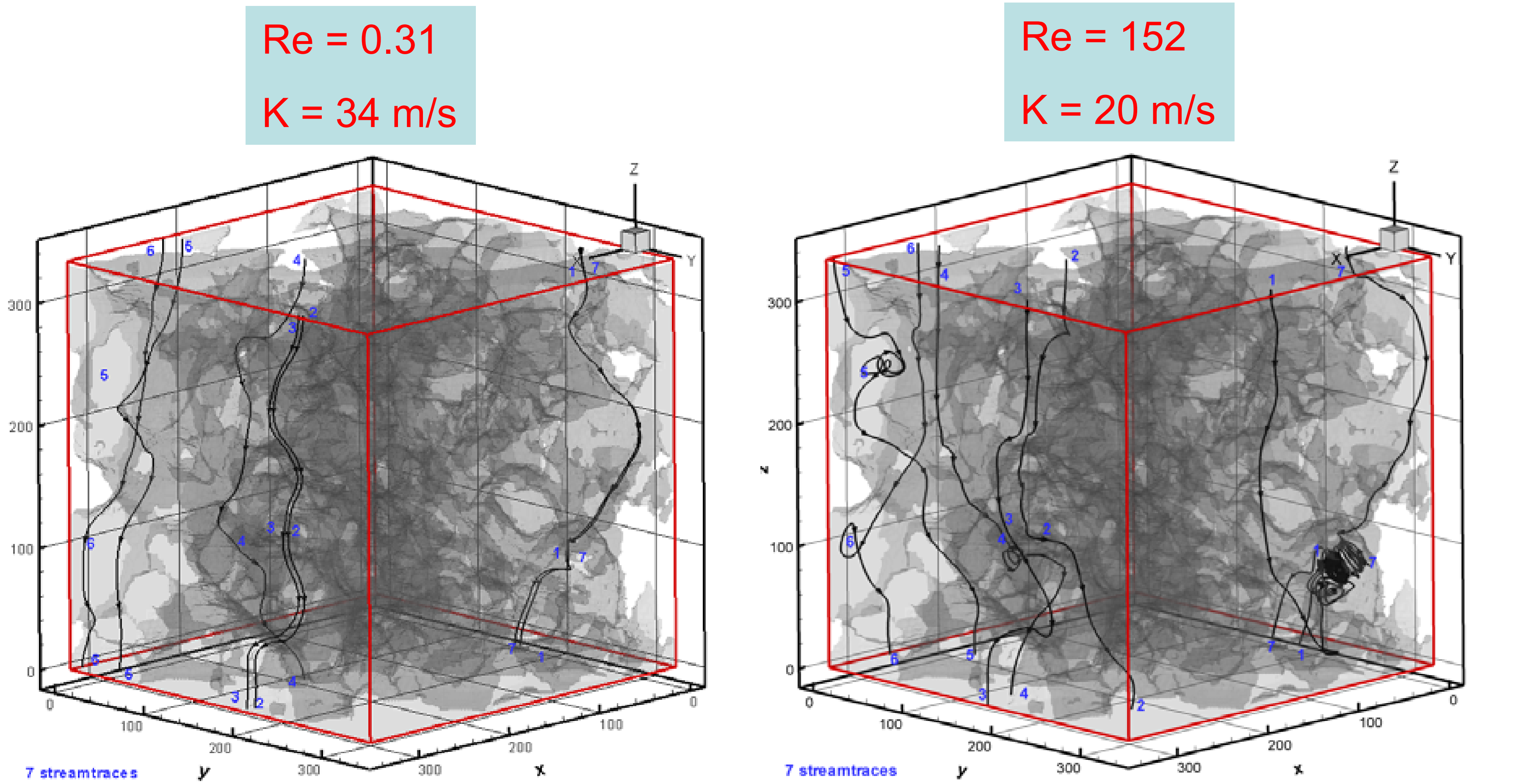

- Streamlines traced forward and backwards from eddy locations and hence begin and end at different locations

Conclusions

- LBM can measure permeabilities outside the range routinely accessible to laboratory measurements
- LBM can assess magnitude of departure from Darcy flow